Jumonji domain-containing protein 6 (Jmjd6) is required for angiogenic sprouting and regulates splicing of VEGF-receptor 1

Jes-Niels Boeckel[a], Virginia Guarani[a], Masamichi Koyanagi[a], Tino Roexe[b], Andreas Lengeling[c], Ralph T. Schermuly[d,e], Pascal Gellert[e], Thomas Braun[e], Andreas Zeiher[b], and Stefanie Dimmeler[a,1]

[a]Institute for Cardiovascular Regeneration, Center of Molecular Medicine, and [b]Division of Cardiology, Department of Medicine III, Goethe University Frankfurt, 60590 Frankfurt, Germany; [c]The Roslin Institute and Royal (Dick) School of Veterinary Studies, University of Edinburgh, Edinburgh EH25 9RG, United Kingdom; [d]Lung Centre, University of Giessen, 35292 Giessen, Germany; and [e]The Max-Planck-Institute for Heart and Lung Research, 61231 Bad Nauheim, Germany

Edited by Louis J. Ignarro, University of California, Los Angeles School of Medicine, Los Angeles, CA, and approved January 13, 2011 (received for review June 9, 2010)

JmjC domain-containing proteins play a crucial role in the control of gene expression by acting as protein hydroxylases or demethylases, thereby controlling histone methylation or splicing. Here, we demonstrate that silencing of Jumonji domain-containing protein 6 (Jmjd6) impairs angiogenic functions of endothelial cells by changing the gene expression and modulating the splicing of the VEGF-receptor 1 (Flt1). Reduction of Jmjd6 expression altered splicing of Flt1 and increased the levels of the soluble form of Flt1, which binds to VEGF and placental growth factor (PlGF) and thereby inhibits angiogenesis. Saturating VEGF or PlGF or neutralizing antibodies directed against soluble Flt1 rescued the angiogenic defects induced by Jmjd6 silencing. Jmjd6 interacts with the splicing factors U2AF65 that binds to Flt1 mRNA. In conclusion, Jmjd6 regulates the splicing of Flt1, thereby controlling angiogenic sprouting.

sFlt1 | hypoxia

The growth of new blood vessels is essential to maintain the oxygen supply, but also needs to be tightly controlled to prevent pathological angiogenesis (1). A subfamily of proteins containing the JmjC domain recently emerged as critical regulators that epigenetically control gene expression. JmjC domain-containing proteins catalyze Fe(II) and 2-oxogluarate–dependent hydroxylation or dioxygenase reactions and, therefore, are regulated by oxygen tension (2). First evidence that these enzymes might control hypoxia responses was provided by studies showing that a member of JmjC domain-containing proteins, the "factor inhibiting hypoxia inducible factor 1" (FIH-1) regulates the recruitment of the transcriptional coactivators of hypoxia-inducible factor 1α (HIF1α) (3, 4). On the other hand, hypoxia was shown to up-regulate the transcription of some of the JmjC domain-containing enzymes, especially of those demonstrated to be involved in histone demethylation (5–10). However, the function of JmjC domain-containing proteins in angiogenesis is largely unknown. Therefore, we investigated whether one of the members of this family of enzymes, Jumonji domain-containing protein 6 (Jmjd6), might be involved in the regulation of angiogenesis. Jmjd6 was first thought to be a cell-surface receptor responsible for the recognition and phagocytosis of apoptotic cells (11). However, various following studies showed that Jmjd6 is localized in the nucleus (12–16) and is not involved in apoptotic cell clearance (17). Subsequently, a function as a histone arginine demethylase was identified (18) and a recent publication suggests that Jmjd6 regulates splicing by hydroxylating the splicing factor U2AF65 (19). Mice lacking Jmjd6 expression die perinatally and display cardiac developmental defects; however, it is unclear whether these mice have intrinsic defects of cells comprising the vasculature (17, 20). Therefore, we investigated the cell intrinsic function of Jmjd6 and its regulation in endothelial cells (ECs).

Results

Functions of Jmjd6 in Endothelial Cells. To investigate the function of Jmjd6 in ECs, Jmjd6 was silenced with siRNAs. Small interfering RNAs directed against Jmjd6 reduced endothelial sprouting in spheroid assays (Fig. 1 *A* and *B*). Moreover, Jmjd6 silencing reduced network formation in a Matrigel assay in vitro (Fig. 1 *C* and *D*) and inhibited invasion of ECs (Fig. 1*E*). The survival of ECs was not affected, despite efficient Jmjd6 reduction (Fig. 1 *A* and *F* and Fig. S1). Conversely, overexpression of wild-type Jmjd6 enhanced sprouting angiogenesis (Fig. 1*G*).

Functions of Jmjd6 in Vivo. We also investigated the in vivo relevance of the findings by using $Jmjd6^{+/-}$ mice, which are viable. Consistent with the inhibition of angiogenesis in vitro, angiogenic sprouting was suppressed in Matrigel plugs that had been implanted in $Jmjd6^{+/-}$ mice (Fig. 2 *A–D*). Additionally, we intravenously infused FITC-conjugated lectin to determine the number of perfused capillaries. Matrigel plugs implanted in $Jmjd6^{+/-}$ mice showed significantly lower number of FITC-lectin–positive areas (Fig. 2 *A–C*). Similar results were obtained when Matrigel plugs were supplemented with bFGF to further enhance angiogenesis (37.7 ± 11% reduction in $Jmjd6^{+/-}$ mice) (Fig. 2 *B* and *C*). Moreover, the dysfunction of ECs was confirmed by demonstrating that cultured lung ECs derived from $Jmjd6^{+/-}$ mice exhibited impaired network forming activity ex vivo compared with cells isolated from wild-type mice (Fig. 2*E*).

Former Functions of Jmjd6. Jmjd6 was suggested to act as a histone arginine demethylase (18). Therefore, we sought to determine the influence of Jmjd6 silencing on histone arginine methylation. However, Jmjd6 silencing in ECs did not affect arginine methylation at H4R3 (Fig. S2).

Jmjd6 Affects Splicing of Angiogenesis-Related Genes in ECs. To address the mechanism by which Jmjd6 affects angiogenic sprouting, we next determined the effect on gene expression by using Affymetrix exon arrays, which allow detecting differences in gene

Author contributions: J.-N.B., M.K., A.Z., and S.D. designed research; J.-N.B., V.G., T.R., and R.T.S. performed research; A.L. contributed new reagents/analytic tools; J.-N.B., P.G., and T.B. analyzed data; and J.-N.B. and S.D. wrote the paper.

The authors declare no conflict of interest.

This article is a PNAS Direct Submission.

[1]To whom correspondence should be addressed. E-mail: dimmeler@em.uni-frankfurt.de.

This article contains supporting information online at www.pnas.org/lookup/suppl/doi:10.1073/pnas.1008098108/-/DCSupplemental.

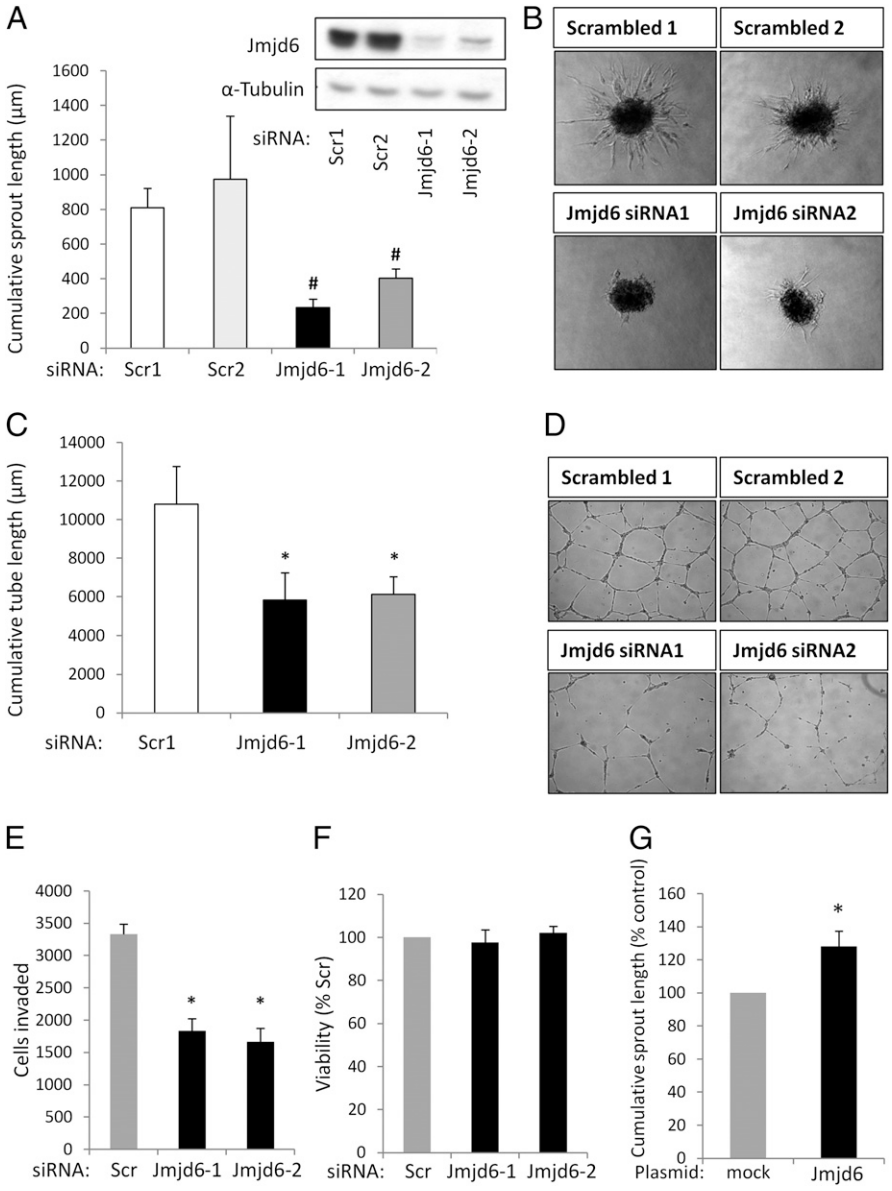

Fig. 1. Regulation of angiogenic sprouting by Jmjd6. (*A–D*) Jmjd6 was silenced in human umbilical vein endothelial cells (HUVECs) by two different siRNAs (Jmjd6-1 and -2) and the functional activity of the cells was compared to two control siRNAs (Scr1 and Scr2). (*A* and *B*) Angiogenic sprouting was compared in the spheroid model. Data are mean ± SEM for $n = 3–4$; $^{\#}P < 0.05$ vs. Scr1 (Mann-Whitney *U* test). (*C* and *D*) In addition, the Matrigel network assay was determined in vitro. Data are mean ± SEM for $n = 4$; $^{*}P < 0.05$ vs. Scr1 (Student's *t* test). (*Inset* in *A*) Knock-down of Jmjd6 protein in siRNA treated cells by Western blot 48 h after transfection. (*E*) Invasion of HUVEC was determined in modified Boyden chambers. Data are mean ± SEM for $n = 3$; $^{*}P < 0.05$ vs. Scr (Student's *t* test). (*F*) Cell viability was measured by MTT cell viability assay. Data are mean± SEM for $n = 3$. (*G*) Assessment of spheroid sprouting in HUVEC overexpressing Jmjd6 plasmid. Data are mean ± SEM for $n = 3$ (Student's *t* test) $^{*}P < 0.05$.

expression as well as splicing. Indeed, Jmjd6 silencing profoundly reduced expression of several genes that are well known to play an important role in ECs, whereas typical angiogenesis inhibitors, such as the Notch ligand Delta-like 4 (Dll4) and SEMA3A, were significantly increased (Fig. 3*A*, and Tables S1 and S2). The dysregulation of some of the genes was validated by qPCR (Fig. 3 *A* and *B*).

Interestingly, bioinformatic assessment of alternative splice variants revealed that Jmjd6 silencing affects the splicing of the *VEGF receptor 1* (*Flt1*) (Table S3). Differential splicing of *Flt1* was shown to generate a soluble form of Flt1 (sFlt1), which binds to the VEGF and the placenta growth factor (PlGF), and thereby inhibits angiogenesis (21–23). By using TaqMan probes designed to detect the boundary between exon 13 and intron 13, allowing the measurement of the Flt1 splice variants that retain intron 13 encoding a premature Stop codon (Fig. S3), we confirmed that silencing of Jmjd6 in ECs increased the splice variant sFlt1-13 (Fig. 3*C*). These results were confirmed by Northern blot (Fig. 3*D*) and splice variant-specific PCRs (Fig. S4). To exclude that the increase in sFlt1 is only secondary to the increased transcription of the full-length membrane form of Flt1 (mFlt1), we additionally determined the ratio of sFlt1/mFlt1 and demonstrated that the ratio is also increased in Jmjd6 siRNA-treated human umbilical vein endothelial cells (HUVECs) (Fig. 3*E*).

Jmjd6-Regulated Splicing Is Dependent on Oxygen. The hydroxylation reaction of Jmjd6 critically depends on the oxygen concentration; hence Jmjd6 is expected to be inhibited under conditions of severe hypoxia (19). Therefore, we investigated the effect of hypoxia on sFlt1 expression. Exposure of ECs with an iron chelator (desferrioxamine, DFO) or hypoxia increased sFlt1 expression and the ratio of sFlt1/mFlt1 in vitro to a similar extent as Jmjd6 siRNA (Fig. 3 *F* and *G*). A similar response was observed in mice, which were exposed to hypoxia (Fig. S5). Taken together, these data demonstrate that sFlt1 levels were increased at 24 h after reducing the oxygen concentration.

Recovery of the Inhibited Angiogenic Phenotype After Jmjd6 Knockdown by Neutralizing Antibodies or Saturating the Level of the Ligands. To determine whether the modulation of splicing leading to increased sFlt1 levels contributes to the angiogenesis suppressive effect induced by Jmjd6 silencing, we incubated Jmjd6 siRNA-

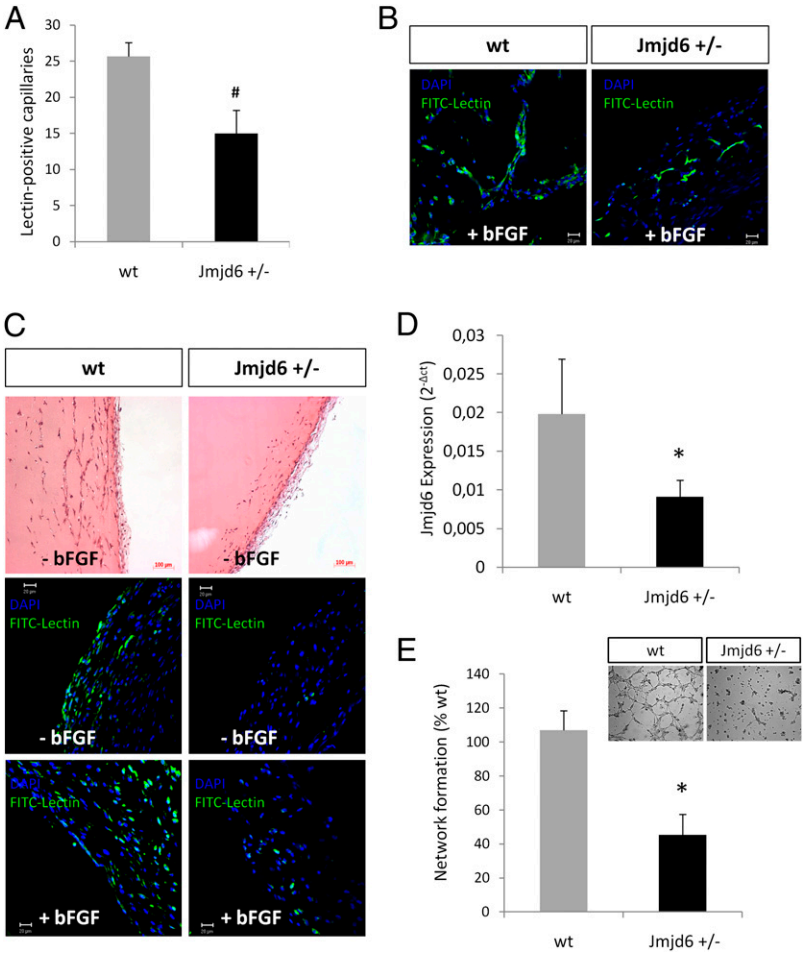

Fig. 2. Angiogenesis in *Jmjd6*$^{+/-}$ mice. (*A*–*C*) Matrigel plugs were subcutaneously implanted in *Jmjd6*$^{+/-}$ mice or wild-type littermates. After 7 d, FITC-lectin was injected and plaque angiogenesis was measured. (*A*) Quantitative analysis of lectin-perfused capillaries. Data are mean ± SEM for $n = 4$ animals/group. $^{\#}P < 0.05$ vs. wild-type (Mann-Whitney *U* test). (*B* and *C*) Representative histological images. (*B*) Higher magnification images in bFGF-supplemented plugs. (Scale bar, 20 μm.) (*C*) Lower magnification images in H&E staining (*Top*), FITC-lectin positive vessel invading in Matrigel plugs with (*Bottom*) or without (*Middle*) bFGF supplementation. [Scale bars, (*Top*) 100 μm, (*Middle* and *Bottom*) 20 μm.] (*D*) Jmjd6 expression in heart tissue of wild-type or *Jmjd6*$^{+/-}$ mice. Data are mean ± SEM for $n = 6$–7 animals (Student's *t* test). (*E*) Lung endothelial cells (ECs) were isolated of wild-type and *Jmjd6*$^{+/-}$ mice and were cultured in Matrigel. Quantification of the network formation is shown. (*Inset*) *A* representative result. Data are mean± SEM for $n = 6$–7 animals. $^{*}P < 0.05$ compared with wild-type (Student's *t* test).

treated cells with saturating concentrations of VEGF or PlGF or both. Saturating concentrations of VEGF or PlGF or both rescued the defective sprouting activity in Jmjd6 silenced ECs (Fig. 4*A*). Moreover, neutralizing antibodies directed against sFlt1 largely compensated the reduced sprouting of Jmjd6 siRNA-transfected cells (Fig. 4*B*), indicating that the increased extracellular concentration of sFlt1 indeed contributes to the anti-angiogenic effects seen after Jmjd6 siRNA treatment.

Jmjd6 Mediates Splicing of *Flt1* by Interacting with U2AF65. Jmjd6 was recently reported to hydroxylate the splicing factor U2AF65 (19). Therefore, we investigated whether U2AF65 might mediate *Flt1* splicing and bind to Flt1 mRNA. Immunoprecipitated U2AF65 binds to sFlt1 mRNA but not to U1 snRNA, which was used as a negative control (Fig. 5*A*). Moreover, Jmjd6 coimmunoprecipitated with U2AF65 (Fig. 5*B*), further supporting a link between Jmjd6 and U2AF65-mediated splicing of *Flt1*.

Discussion

Reducing the expression of Jmjd6 by siRNA-mediated silencing in vitro or in transgenic mouse models resulted in impaired sprouting angiogenesis. We further demonstrate that Jmjd6 expression controls splicing of *Flt1*. Jmjd6 silencing augmented the expression of the alternative splice variant of *Flt1* that contains exons 1 to 13 of *Flt1*, leading to the generation of a protein that lacks the transmembrane and intracellular kinase domain, hence functioning as a soluble VEGF- and PlGF-trapping molecule. Soluble Flt1 was initially cloned in 1993 (24) and, since then, additional splice variants that terminate with exon 14 and exon 15a or 15b have been identified, some of which are specifically expressed in smooth-muscle cells (25–27). Although the detailed biological and molecular functions remain to be determined, increasing evidence suggest that sFlt1 is up-regulated by hypoxia in the placenta and plays a causal role in the pathogenesis of preeclampsia (28, 29). Moreover, therapeutic application of sFlt1 has been tested in disease models of abnormal angiogenesis, for example, in retinopathy (30). In the present study, we demonstrate that Jmjd6 silencing leads to increased sFlt1 mRNA expression, resulting in higher levels of the secreted protein in cell-culture supernatants. Neutralizing sFlt1 antibodies or saturating VEGF or PlGF ameliorate the angiogenesis inhibition in Jmjd6 siRNA-treated cells. These data confirm that the increase in sFlt1 causally contributes to the angiogenesis impairment seen in the in vitro Jmjd6-silencing experiments. However, this finding does not exclude that Jmjd6 exhibits additional functions. Consistent with other studies evaluating histone modifications by mass spectrometry (19), we did not see global changes in histone methylation patterns in Jmjd6-deficient cells. However, these experiments do not rule out that histone modifications might be changed at specific promoters. Moreover, our gene expression arrays document profound changes in the expression of key angiogenesis regulators in Jmjd6-silenced ECs that may disturb coordinated sprouting angiogenesis in addition to the dysregulation of sFlt1 levels. One may speculate that the modulation of sFlt1 levels may biologically control the proangiogenic factors PlGF and VEGF, thereby coordinating vessel growth and maturation. Taken together, our data provide evidence that Jmjd6 may act as a molecular sensor coupling oxygen levels to coordinated endothelial responses in order to meet the metabolic demands of the hypoxic tissues.

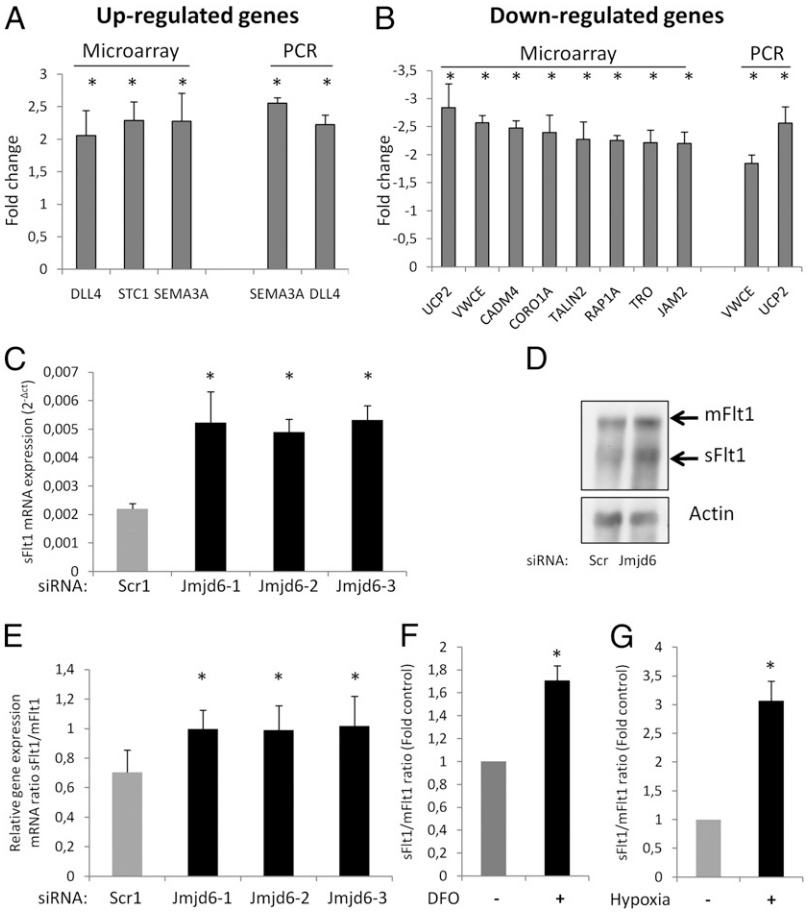

Fig. 3. Modulation of gene expression and splicing by Jmjd6. (*A* and *B*) Jmjd6 was silenced by siRNA in HUVEC and gene expression and splicing was determined by GeneChip Human Exon 1.0 ST array 48 h after siRNA transfection. Data are mean ± SEM for $n = 3$ independent experiments. Selection of significantly up-regulated (*A*) or down-regulated genes (*B*). Selected genes were confirmed by qPCR, as shown in the right panel of the figures. Data are mean ± SEM for $n \geq 3$. *$P < 0.05$ vs. Scr. (Student's *t* test). (*C*) Soluble Flt1 expression in Jmjd6 siRNA-treated HUVECs. Data are mean ± SEM for $n = 3$ independent experiments. *$P < 0.05$ vs. control siRNA (Student's *t* test). (*D*) Jmjd6 expression was silenced by siRNA in ECs. Forty-eight hours after transfection, a Northern blot was used to detect the alternative splicing forms of the Flt1 mRNA; mFlt1 and sFlt1 are indicated by arrows. A reprobe with an actin probe served as a loading control. (*E*) Ratio of sFlt1/mFlt1 expression in Jmjd6 siRNA-treated HUVECs. Data are mean ± SEM for $n = 3$ independent experiments. *$P < 0.05$ vs. normoxia (Student's *t* test). (*F*) Ratio of sFlt1/mFlt1 expression after incubation of HUVECs with 50 μM DFO for 24 h was detected by qPCR. Data are mean ± SEM for $n = 4$; *$P < 0.05$ vs. control. (Student's *t* test). (*G*) Ratio of sFlt1/mFlt1 expression after incubation of HUVECs under hypoxia (0.1% O_2) for 24 h was detected by qPCR. Data are mean ± SEM for $n = 3$. *$P < 0.05$ vs. normoxia (Student's *t* test).

Materials and Methods

Cell Culture. Pooled HUVECs were purchased from Cambrex and cultured in endothelial basal medium (EBM; Cambrex) supplemented with 1 μg/mL hydrocortisone, 3 μg/mL bovine brain extract, 30 μg/mL gentamicinsulfat, 50 μg/mL amphotericin B, 10 μg/mL EGF (all Lonza), and 10% FCS (Gibco) on culture dishes until the third passage. After detachment with trypsin, cells were grown in 6-cm culture dishes (Greiner) or T75 flasks (Greiner) for at least 24 to 48 h.

RNA Analysis. Total RNA was isolated using Quiazol (79306; Qiagen) and miRNeasy-kit (217004; Qiagen) with additional DNase I (79254; Qiagen) digestion according to the manufacturer's protocol. Afterward, 1 μg of RNA from each sample was reverse-transcribed into random hexamer primed single-strand cDNA (10 min at 25 °C, 15 min at 42 °C, 5 min at 99 °C) by M-MLV Reverse Transcriptase (N8080018; Invitrogen) and subjected to qPCR using the StepOnePlus Real-Time PCR System (Applied Biosystems). The sequences of the primer sets and probes for PCR are available upon request.

Plasmid Constructs and Transfection. HUVECs were grown in a 6-cm well to 60–70% confluence and then transfected with 6 μg of plasmids. Empty vector: pFlag-CMV-6a-BAP (C-5722; Sigma) and the Jmjd6-containing plasmid: pFlag-CMV-6a-Jmjd6. Transfection was performed using the Targetfect F2 and Virofect reagents (Targeting Systems) according to the manufacture's protocol for HUVEC transfection, as described previously (31).

Small Interfering RNA Knockdown. For siRNA-mediated gene silencing, HUVECs were grown to 60–70% confluence and transfected with GeneTrans II. Cells were transfected with Jmjd6 siRNA I (5′-GAGGGAACCAGCAAGACGA-3′), Jmjd6 siRNA II (5′-CCUGGAAUGCCUUAGUUCA-3′), Jmjd6 siRNA III (5′-GUGUGGUGAGGAUAACGAU-3′). Scrambled-I (5′-UCUCUCACAACGGGCAUUU-3′) or scrambled-II (5′-GUGGGCACCGAUAUCUUGATT-3′) siRNA was used as a control (all Sigma Aldrich), all in a final concentration of 60 nM for 48 h.

Splice-Specific PCR. Primers and PCR conditions were used as previously described (24). Specifically, three primers were used: Flt-1-F (5′-GCACCTTGGTTGTGGCTGAC-3′), sFlt-3-R (5′-CAACAAACACAGAGAAGG-3′), Flt-2-R (5′-

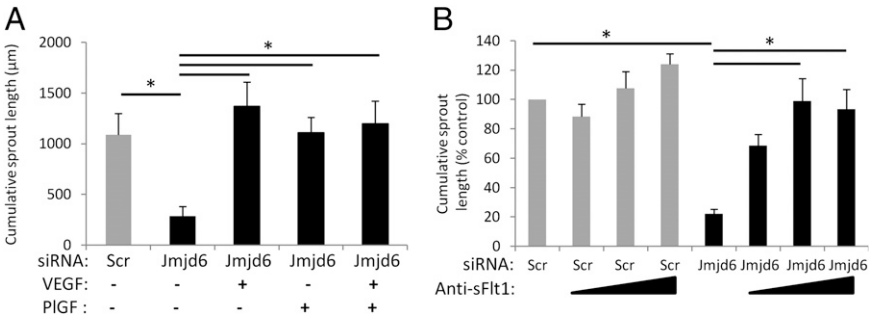

Fig. 4. Rescue of Jmjd6 silencing mediated impaired sprouting angiogenesis. (*A* and *B*) Jmjd6 was silenced by siRNA and angiogenic sprouting was determined using the spheroid assay in the presence or absence of recombinant VEGF, PlGF, or VEGF/PlGF heterodimer (*A*) or neutralizing anti-sFlt1 antibody (*B*). Data are mean ± SEM for $n = 3$–4. Five or more spheroids were counted per experiment. *$P < 0.05$ (ANOVA).

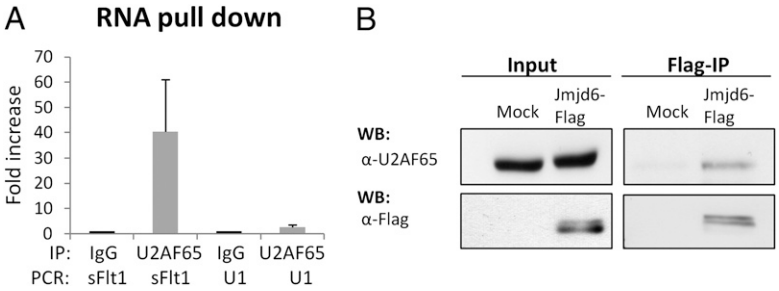

Fig. 5. Jmjd6 mediates splicing of *Flt1* by interacting with U2AF65. (*A*) U2AF65 was immunoprecipitated and bound RNA was quantified by qPCR for sFlt1 or the control RNA U1. Data are mean ± SEM for $n = 3$ independent experiments. (*B*) Jmjd6-Flag was immunoprecipitated and bound U2AF65 was detected by Western blot. Three percent of the Lysates were loaded as input control.

TGGAATTCGTGCTGCTTCCTGGTCC-3′) to detect a 747-bp product (sFlt1) and a 549-bp product (mFlt1).

Northern Blot. Total RNA was fractionated on a 1% formaldehyde agarose gel, transferred to nylon membranes (11209272001; Roche) by capillary blotting and hybridized at 40 °C overnight, with 9 μg/mL of a digoxigenin (DIG)-labeled DNA probe (Flt1-Exon13-DIG-Sonde: 5′-DIG-AGTTTCAGG-TCCTCTCCTTC-3′; Sigma) against Flt1 and sFlt1 in "DIG Easy Hyp" hybridization buffer (Roche). Actin RNA probe was purchased from Roche. The mRNA was detected using the "DIG Luminescent Detection Kit" (Roche) according to the manufacturer's protocol.

RNA Immunoprecipitation Assay. RNA immunoprecipitation was performed using HUVEC lysates. For each immunoprecipitation 20×10^6 cells were used and either 5 μg anti-U2AF65 (mouse monoclonal, U4758; Sigma) or 5 μg mouse IgG (cs200621; Millipore) were added. Further steps were done using the EZ-Magna RIP Kit (17–701; Millipore) according to the manufacturer's protocol. Bound RNA was then detected by qPCR using Taqman probes specific for sFlt1 or primers for U1 snRNA as a control.

Microarray Analysis. Gene-expression profiling was performed using the GeneChip Human Exon 1.0 ST array (Affymetrix). RNA isolation was done as described above and the microarray processing was carried out by ATLAS biolabs (Germany). Data were analyzed by using the Exon Array Analyzer (EAA) Web interface (32). The raw CEL files were processed by RMA (33) for background correction and estimation of exon and gene signals. Probes, which are targeting to putative exonic regions because of prediction algorithms (full annotation set), were excluded from our analysis (Affymetrix, Inc.). Furthermore, the "Detection Above Background (DABG)" algorithm (Affymetrix Inc.) was used to identify signals within the background noise. Exon arrays tend to false-positive results (34), which can be reduced by EAA because of various filters (32). The most important filter exclude exons that are not expressed in both groups, genes that are not expressed in either groups, as well as probe sets that are known to cross-hybridize. For our analysis, parameters for all available filters were left on default settings of EAA. To identify differentially expressed exons between two groups, it has to be considered that also the expression of the gene can differ between groups. By normalizing each exon signal by the expression of the gene, the signals can be compared directly. The Splice Index (34) is the logarithmic fold change of the normalized exon signals. In addition, Student's *t* test was used to identify statistical differences.

Western Blot Analysis. For Western blot analysis, HUVECs were lysed in RIPA lysis buffer (Sigma) for 20 min on ice. After centrifugation for 15 min at $14{,}000 \times g$ (4 °C), the protein content of the samples was determined according to the Bradford method. Equal amounts of protein were loaded onto SDS-polyacrylamide gels and blotted onto PVDF membranes (IPFL00010; Millipore). Western blots were performed by using antibodies directed against Jmjd6 (1:250, H-7, Sc-28348; Santa Cruz), U2AF65 (1:1,000, U4758; Sigma), $H4R3me2_{(sym)}$ (1:500, 39275; Active Motif), α-Tubulin (1:4,000, MS-581-P1; NeoMarkers), or Histone H4 (1:1,000, ab31827-100; Abcam).

Immunoprecipitation Assay. For immunoprecipitation, cells were either transfected with Jmjd6-Flag or GFP-expressing vectors; 24 h after transfection immunoprecipitation was performed using the FLAG Immunoprecipitation Kit (FLAGIPT1; Sigma) in accordance with manufacturer's protocol. Immunoprecipitates and input controls (3% of the lysates) were subjected to SDS/PAGE, and probed first with antibodies against U2AF65 (1:1,000, U4758; Sigma) and then reprobed against the Flag-epitop (1:1,000, A8592; Sigma).

MTT Viability Assay. Assessment of cell viability was performed using the MTT [3-(4,5-dimethylthiazol-2-yl)-2,5-diphenyl-2H-tetrazolium bromide] assay. Forty-eight hours after transfection, 0.5 mg/mL MTT was added to each well and cells were incubated for 4 h at 37 °C. Cells were washed with PBS and lysed 30 min at room temperature with lysis buffer (40 nM HCl in isopropanol). Absorbance was photometrically measured at 550 nm.

In Vitro Hypoxia Experiments. HUVECs ($6 \times 10^4/cm^2$) were cultured in a 6-cm dish (Greiner Bio-One). After 24 h, cells were incubated at 0.1% O_2 for 24 h. For the DFO experiment, 3×10^5 cells were cultured in a 6-cm dish (Greiner Bio-One) for 24 h, then 50 μM DFO was added for additional 24 h.

Tube Formation Assay. Twenty-four hours after transfection, HUVECs (2×10^5) were cultured in a 12-well plate (Greiner) coated with 200 μL Matrigel Basement Membrane Matrix (BD Biosciences). Tube length was quantified after 24 h by measuring the cumulative tube length in five random microscopic fields with a computer-assisted microscope using Axiovision 4.5 (Zeiss).

Spheroid-Based Angiogenesis Assay. EC spheroids of defined cell number were generated as described previously (35). In recovery experiments, VEGF (30 ng/mL), PlGF (30 ng/mL), or VEGF/PlGF-heteromer (30 ng/mL) (all R&D) or 1, 2, or 5 μg/mL of neutralizing anti-VEGFR1 (soluble) antibodies (Invitrogen; 36–1100) was added. In vitro angiogenesis was quantified by measuring the cumulative length of the sprouts that had grown out of each spheroid using a digital imaging software (Axioplan; Zeiss) analyzing 10 spheroids per group per experiment.

Invasion Assay. To assess the invasion capacity of HUVEC with reduced Jmjd6 expression, a total of 3×10^5 HUVECs were resuspended in 200 μL EBM medium (Lonza) supplemented with 1% BSA (PAA) and placed in the upper chamber (Falcon, 8-μm pore size) coated with 50 μL Matrigel (Becton-Dickinson). Then, the chamber was placed in a 24-well culture dish (Falcon) containing 500 μL EBM supplemented with 10% FCS (Gibco) and single quots (Lonza). After 24 h of incubation at 37 C°, transmigrated cells were counted manually in five random microscopic fields.

In Vitro Tube Formation of Lung ECs. Isolation of murine ECs was performed as described previously (31). Murine lung ECs (2×10^5) were cultured in a 12-well plate (Greiner) coated with 200 μL Matrigel Basement Membrane Matrix (BD Biosciences). Tube length was quantified after 24 h by measuring the cumulative tube length in three random microscopic fields with a computer-assisted microscope using Axiovision 4.5 (Zeiss).

***Jmjd6* Knockout Mice.** The generation of the *Jmjd6* knockout mice used in this study was previously described, including the primer sequences for genotyping (17).

In Vivo Matrigel Experiments. Eight-wk-old mice were injected subcutaneously with two Matrigel Basement Matrix plugs at day 0 mixed with or without 0.5 μg/mL bFGF. Tissue and Matrigel plugs were harvested 7 d after implantation. To analyze perfused capillaries, 200 μL FITC-conjugated lectin (1 mg/mL) was injected intravenously 30 min before harvest or plug sections were stained using H&E. For quantification of perfused vessels, lectin-positive capillaries were counted.

In Vivo Hypoxia Experiments. All experiments were performed using adult male mice (8-wk-old C57BL/6) according to the institutional guidelines that comply with national and international regulations. The experiments have been approved by the local ethics committee (Regierungspräsidium Darmstadt). Mice were exposed to chronic hypoxia (10% O_2) for 24 h in a ventilated chamber, as described previously (36). The level of hypoxia was held constant by an auto regulatory control unit (model 4010, O_2 controller;

Labotect) supplying either nitrogen or oxygen. The chamber temperature was maintained at 22 to 24 °C. Control animals were kept in identical chambers under normoxic condition.

Statistical Analysis. Data are expressed as mean ± SEM. Two treatment groups were compared by Mann-Whitney *U* test or Student´s *t* test (Graphpad Software, Inc.). Multiple group comparisons were done by ANOVA (post hoc analysis). Results were considered statistically significant when $P < 0.05$.

ACKNOWLEDGMENTS. This study was supported by the Deutsche Forschungsgemeinschaft (TR-SFB23 project B5 and Exc147/1).

1. Carmeliet P (2005) Angiogenesis in life, disease and medicine. *Nature* 438:932–936.
2. Tsukada Y, et al. (2006) Histone demethylation by a family of JmjC domain-containing proteins. *Nature* 439:811–816.
3. Hewitson KS, et al. (2002) Hypoxia-inducible factor (HIF) asparagine hydroxylase is identical to factor inhibiting HIF (FIH) and is related to the cupin structural family. *J Biol Chem* 277:26351–26355.
4. Lando D, et al. (2002) FIH-1 is an asparaginyl hydroxylase enzyme that regulates the transcriptional activity of hypoxia-inducible factor. *Genes Dev* 16:1466–1471.
5. Pollard PJ, et al. (2008) Regulation of Jumonji-domain-containing histone demethylases by hypoxia-inducible factor (HIF)-1alpha. *Biochem J* 416:387–394.
6. Wellmann S, et al. (2008) Hypoxia upregulates the histone demethylase JMJD1A via HIF-1. *Biochem Biophys Res Commun* 372:892–897.
7. Sar A, Ponjevic D, Nguyen M, Box AH, Demetrick DJ (2009) Identification and characterization of demethylase JMJD1A as a gene upregulated in the human cellular response to hypoxia. *Cell Tissue Res* 337:223–234.
8. Beyer S, Kristensen MM, Jensen KS, Johansen JV, Staller P (2008) The histone demethylases JMJD1A and JMJD2B are transcriptional targets of hypoxia-inducible factor HIF. *J Biol Chem* 283:36542–36552.
9. Krieg AJ, et al. (2010) Regulation of the histone demethylase JMJD1A by hypoxia-inducible factor 1 alpha enhances hypoxic gene expression and tumor growth. *Mol Cell Biol* 30:344–353.
10. Xia X, et al. (2009) Integrative analysis of HIF binding and transactivation reveals its role in maintaining histone methylation homeostasis. *Proc Natl Acad Sci USA* 106: 4260–4265.
11. Fadok VA, et al. (2000) A receptor for phosphatidylserine-specific clearance of apoptotic cells. *Nature* 405:85–90.
12. Cikala M, et al. (2004) The phosphatidylserine receptor from Hydra is a nuclear protein with potential Fe(II) dependent oxygenase activity. *BMC Cell Biol* 5:26.
13. Cui P, Qin B, Liu N, Pan G, Pei D (2004) Nuclear localization of the phosphatidylserine receptor protein via multiple nuclear localization signals. *Exp Cell Res* 293:154–163.
14. Krieser RJ, et al. (2007) The *Drosophila* homolog of the putative phosphatidylserine receptor functions to inhibit apoptosis. *Development* 134:2407–2414.
15. Mitchell JE, et al. (2006) The presumptive phosphatidylserine receptor is dispensable for innate anti-inflammatory recognition and clearance of apoptotic cells. *J Biol Chem* 281:5718–5725.
16. Tibrewal N, Liu T, Li H, Birge RB (2007) Characterization of the biochemical and biophysical properties of the phosphatidylserine receptor (PS-R) gene product. *Mol Cell Biochem* 304:119–125.
17. Böse J, et al. (2004) The phosphatidylserine receptor has essential functions during embryogenesis but not in apoptotic cell removal. *J Biol* 3(4):15.
18. Chang B, Chen Y, Zhao Y, Bruick RK (2007) JMJD6 is a histone arginine demethylase. *Science* 318:444–447.
19. Webby CJ, et al. (2009) Jmjd6 catalyses lysyl-hydroxylation of U2AF65, a protein associated with RNA splicing. *Science* 325(5936):90–93.
20. Schneider JE, et al. (2004) Identification of cardiac malformations in mice lacking Ptdsr using a novel high-throughput magnetic resonance imaging technique. *BMC Dev Biol* 4(1):16.
21. Maynard SE, et al. (2003) Excess placental soluble fms-like tyrosine kinase 1 (sFlt1) may contribute to endothelial dysfunction, hypertension, and proteinuria in preeclampsia. *J Clin Invest* 111:649–658.
22. Wu FT, et al. (2010) A systems biology perspective on sVEGFR1: Its biological function, pathogenic role and therapeutic use. *J Cell Mol Med* 14:528–552.
23. Olsson AK, Dimberg A, Kreuger J, Claesson-Welsh L (2006) VEGF receptor signalling—In control of vascular function. *Nat Rev Mol Cell Biol* 7:359–371.
24. Kendall RL, Thomas KA (1993) Inhibition of vascular endothelial cell growth factor activity by an endogenously encoded soluble receptor. *Proc Natl Acad Sci USA* 90: 10705–10709.
25. Thomas CP, Andrews JI, Liu KZ (2007) Intronic polyadenylation signal sequences and alternate splicing generate human soluble Flt1 variants and regulate the abundance of soluble Flt1 in the placenta. *FASEB J* 21:3885–3895.
26. Sela S, et al. (2008) A novel human-specific soluble vascular endothelial growth factor receptor 1: Cell-type-specific splicing and implications to vascular endothelial growth factor homeostasis and preeclampsia. *Circ Res* 102:1566–1574.
27. Heydarian M, et al. (2009) Novel splice variants of sFlt1 are upregulated in preeclampsia. *Placenta* 30:250–255.
28. Thomas CP, et al. (2009) A recently evolved novel trophoblast-enriched secreted form of fms-like tyrosine kinase-1 variant is up-regulated in hypoxia and preeclampsia. *J Clin Endocrinol Metab* 94:2524–2530.
29. Wu FT, et al. (2010) A systems biology perspective on sVEGFR1: Its biological function, pathogenic role and therapeutic use. *J Cell Mol Med* 14:528–552.
30. Bainbridge JW, et al. (2002) Inhibition of retinal neovascularisation by gene transfer of soluble VEGF receptor sFlt-1. *Gene Ther* 9:320–326.
31. Potente M, et al. (2007) SIRT1 controls endothelial angiogenic functions during vascular growth. *Genes Dev* 21:2644–2658.
32. Gellert P, Uchida S, Braun T (2009) Exon Array Analyzer: A web interface for Affymetrix exon array analysis. *Bioinformatics* 25:3323–3324.
33. Irizarry RA, et al. (2003) Exploration, normalization, and summaries of high density oligonucleotide array probe level data. *Biostatistics* 4:249–264.
34. Clark TA, et al. (2007) Discovery of tissue-specific exons using comprehensive human exon microarrays. *Genome Biol* 8:R64.
35. Korff T, Augustin HG (1998) Integration of endothelial cells in multicellular spheroids prevents apoptosis and induces differentiation. *J Cell Biol* 143:1341–1352.
36. Schermuly RT, et al. (2007) Phosphodiesterase 1 upregulation in pulmonary arterial hypertension: Target for reverse-remodeling therapy. *Circulation* 115:2331–2339.